ELSEVIER

Journal of Neuroscience Methods 94 (1999) 5–17

JOURNAL OF NEUROSCIENCE METHODS

www.elsevier.com/locate/jneumeth

Multiple single unit recording in the cortex of monkeys using independently moveable microelectrodes

S.N. Baker [a,*,1], N. Philbin [a], R. Spinks [a], E.M. Pinches [a], D.M. Wolpert [a], D.G. MacManus [b], Q. Pauluis [c], R.N. Lemon [a]

[a] *Sobell Department of Neurophysiology, Institute of Neurology, Queen Square, London WC1N 3BG, UK*
[b] *Department of Clinical Neurology, NMR Unit, Institute of Neurology, Queen Square, London WC1N 3BG, UK*
[c] *Laboratory of Neurophysiology, School of Medicine, Université Catholique de Louvain, Brussels, Belgium*

Received 16 April 1999; accepted 1 August 1999

Abstract

Simultaneous recording from multiple single neurones presents many technical difficulties. However, obtaining such data has many advantages, which make it highly worthwhile to overcome the technical problems. This report describes methods which we have developed to permit recordings in awake behaving monkeys using the 'Eckhorn' 16 electrode microdrive. Structural magnetic resonance images are collected to guide electrode placement. Head fixation is achieved using a specially designed headpiece, modified for the multiple electrode approach, and access to the cortex is provided via a novel recording chamber. Growth of scar tissue over the exposed dura mater is reduced using an anti-mitotic compound. Control of the microdrive is achieved by a computerised system which permits several experimenters to move different electrodes simultaneously, considerably reducing the load on an individual operator. Neurones are identified as pyramidal tract neurones by antidromic stimulation through chronically implanted electrodes; stimulus control is integrated into the computerised system. Finally, analysis of multiple single unit recordings requires accurate methods to correct for non-stationarity in unit firing. A novel technique for such correction is discussed.

Keywords: Motor cortex; Monkey; Multiple electrodes; Dura mater; Pyramidal tract; Antidromic identification

1. Introduction

Of all the techniques available for studying the function of the brain at a systems level, recording of neural activity from awake behaving animals is the most direct. Work in slices can provide a wealth of detailed information, but suffers from the disconnection of the studied network from all other brain structures. Work in anaesthetised animals cannot look at the relation of neural activity to behaviour. Studies which use brain scanning of human volunteer subjects (fMRI or PET) can use complex and interesting task configurations, but must read out neural activity levels through the slow and spatially broad filter of the haemodynamic response. Using conventional single electrode penetrations made repeatedly on successive recording days, an impressive wealth of information about the function of the CNS has been built up over the last 40 years (Jasper et al., 1958). However, obtaining such recordings is technically demanding, because successful experiments depend not only on various electronic, surgical and mechanical factors working simultaneously, but also on the good performance of the animal on the trained task (Lemon, 1984).

If such single electrode recordings in awake behaving animals present challenges, those which seek to record the activity from multiple sites at the same time are even harder. It is our firm belief, however, that the benefits of obtaining such recordings greatly outweigh the increased difficulties which must be overcome. Firstly, the yield of data concerning the activity of single neurones during the experimental paradigm can

* Corresponding author. Tel.: +44-1223-333757; fax: +44-1223-334967.
E-mail address: snb11@cam.ac.uk (S.N. Baker)
[1] Present address: Department of Anatomy, University of Cambridge, Cambridge CB2 3DY, UK.

0165-0270/99/$ - see front matter
PII: S0165-0270(99)00121-1

be greatly improved by using a multiple electrode approach. The same number of cells can be gathered in a fraction of the time compared to conventional single electrode recordings. Over the months of recording required with a single electrode, there may be subtle changes in the animal's task performance. Performance is more likely to remain constant over the briefer period required when making multiple electrode recordings.

Most importantly, however, simultaneous recording of many cells permits a wide range of analyses which cannot be carried out otherwise. Such analyses all have in common the computation of covariance between the discharge of different cells. This analysis can be performed over a number of different time scales, providing information on the correlation of neural firing rate (e.g. Lee et al., 1998), or data on short-term synchronisation between the timing of individual spikes (Perkel et al., 1967). The latter has generated increasing interest over the last 10 years, as a number of groups, in a wide range of systems, have provided evidence for a role of such synchrony in neural information coding (Eggermont et al., 1983; Lindsey et al., 1992; Eckhorn, 1994; Singer and Gray, 1995; Vaadia et al., 1995; Riehle et al., 1997; Stopfer et al., 1997; Kilner et al., 1999). Training an animal to perform a behavioural task requires an extensive investment of time and resources, and to justify this investment, it is certainly worthwhile to overcome the technical difficulties and to gather multiple electrode recordings in the final experiment. The wide, and ever expanding, range of analysis techniques for quantifying neural correlation can then be used to obtain the maximum benefit from the valuable experimental data.

In this paper, we will review the system which we have developed recently in London for making multiple single unit recordings from awake behaving monkeys. Although this system was designed to record from the motor cortical areas, it would also be appropriate for recording from other brain structures. The system is based on the Eckhorn microdrive, which is commercially available (Thomas Recording Ltd; Eckhorn and Thomas, 1993), and permits up to 16 independently moveable microelectrodes to be inserted into the cortex. The electrodes have a external shaft diameter of 80 μm, and are made of platinum-iridium insulated with quartz glass. They are positioned in a 4×4 grid, with inter-electrode spacing 330 μm. This geometry, although providing fine-grained sampling of the cortex, results in only 7% of the cortical volume explored being displaced by the electrode array.

We shall describe a number of different technical procedures which facilitate the use of this system and make recording accurate and efficient. Firstly, we have used structural MRI to identify cortical sulci and assist orientation of electrode penetrations in the banks of these sulci. Secondly, we have developed a rigid mounting system for the Eckhorn drive and integrated this with our existing method for implantation of a secure headpiece for head fixation. We have also developed a new chamber for use with the Eckhorn system. Thirdly, we have adopted a new method to deal with the problem of connective tissue growth in the chamber. We describe our approach for controlling many electrodes simultaneously and maximising the yield of high-quality multiple single unit recordings. The cells are identified using antidromic stimulation. Finally, we present a useful technique for removing the effects of non-stationarity in neural firing rates from cross-correlation histograms and spike triggered averages of rectified EMG.

2. Use of structural MRI to guide implants in monkeys

Accurate placement of recording chambers in the monkey is complicated by the variability between animals in sulcal geometry and the stereotaxic location of different cortical areas. We have found structural MRI in the monkey to be of considerable use in guiding the location of recording chambers and in positioning stimulating electrodes in deep brain structures such as the pyramidal tract. It is also particularly helpful in determining the optimal angle of microelectrode penetrations targeted in the banks of deep sulci, such as the central and arcuate sulci.

The main technical difficulty is to avoid any movement during the MRI scan; to achieve this we have used inhalation anaesthetics to provide deep, general anaesthesia. Because of the strong magnetic fields, it important that no metal components come into the vicinity of the scanner. For this reason we scan each monkey before any implantation procedures are carried out.

After induction with ketamine (10 mg kg^{-1} i.m.) the monkey is intubated, and anaesthesia continued by inhalation of Isoflurane ($2-2\frac{1}{2}$%) in 50:50 N_2O:O_2, using an open circuit (Flecknell, 1996). Long (c. 3 m) plastic tubes are used to connect the animal to the anaesthetic trolley; these allow the metal trolley to be kept at a safe distance from the MRI machine. End-tidal pCO_2 is also monitored through an equally long sample tube: this provides a convenient means for remote monitoring of respiratory performance during the scan. ECG is monitored through the scanner's in-built system, and body temperature measured with a mercury-in-glass thermometer. The monkey is wrapped in plastic bubble-wrap to prevent heat loss, and kept warm by bags of saline previously heated in a microwave oven.

Once a stable anaesthetic state is achieved, the head is fixed into a non-metallic (Perspex or Plexiglass) stereotaxic frame. The ear bars of this frame are machined to have a 10 mm outside diameter, tapering to

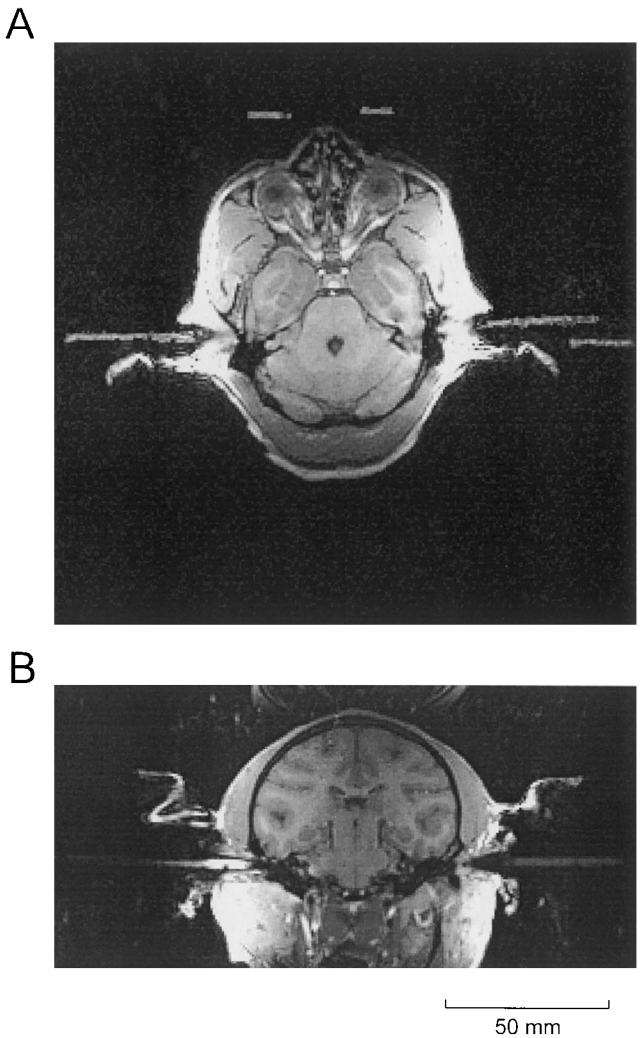

Fig. 1. Example MRI scans from a monkey. (A) Section orientated approximately in the horizontal plane. The vegetable oil markers in the eye bars, placed on the infraorbital margins, and the ear bars in the auditory meatus can be clearly seen. (B) Approximately coronal section showing the ear bars and the location of the central sulcus.

the blunt profile usual for atraumatic ear bars. In the centre of each bar is drilled a 3 mm diameter hole; this runs the length of the ear bar, finishing 3 mm from the end. These holes are filled with vegetable cooking oil, which yields high contrast in MR images. The ends of the holes are threaded to take a nylon screw, which seals them to prevent loss of the oil. When filling the bars, care must be taken to avoid the presence of air bubbles, which will otherwise generate a 'hole' in the high contrast region produced by the oil in the images. The eye bars of the stereotaxic frame likewise are specially machined out of Perspex, and have also have oil-filled holes in them. These oil markers permit later alignment to the stereotaxic co-ordinate frame (see below).

The animal is then moved into the scanner. The pCO_2 meter and gas trolley are placed at a safe distance from the magnet, and positioned so that they can be monitored from outside the shielded room. We perform MRI on a GE Medical Systems Signa Horizon 1.5 Tesla system, with two 3 inch circular receiver coils in a phased array configuration and using spin echo (2D) and gradient echo (3D volume) during data acquisition. Voxel dimensions are 0.7 mm. The whole scan takes about 15 min, after which the animal is returned to the operating theatre, where anaesthesia is discontinued. Once recovery commences, the animal is placed in a recovery cage and monitored in the usual way.

Fig. 1 shows typical images which can be obtained using this procedure. Fig. 1A shows an approximately horizontal section, which includes the plane of the vegetable oil eye and ear bar markers. Fig. 1B shows an approximately coronal section, which includes the ear bar markers and the central sulcus.

The co-ordinates of the eye and ear bar vegetable oil markers should firstly be determined in the scanner reference frame, together with the location of the brain structures of interest. This can be easily performed using software available on the MRI scanner itself. It is then necessary to transform the co-ordinates from these arbitrary axes to stereotaxic space. The transformation required is a translation followed by a rotation, expressed mathematically as:

$$\underline{v} = R(\underline{u} + \underline{k}) \tag{1}$$

where $\underline{u}$ is the three component co-ordinate vector measured from the images, $\underline{k}$ is a translation and $\underline{v}$ is the required co-ordinate of the point in stereotaxic space. In expressing co-ordinates as vectors, a convention must be determined for their ordering (e.g. medio-lateral, anterio-posterior, height), and sign (e.g. left positive, right negative). The actual convention used is quite immaterial, but must be consistent throughout.

R is a three-by-three general rotation matrix about the three co-ordinate axes, and is given by:

$$R = \begin{bmatrix} \cos\beta\cos\gamma & \cos\beta\sin\gamma & \sin\beta \\ \sin\alpha\sin\beta\cos\gamma + \cos\alpha\sin\gamma & \sin\alpha\sin\beta\cos\gamma + \cos\alpha\cos\gamma & -\sin\alpha\cos\beta \\ -\cos\alpha\sin\beta\cos\gamma + \sin\alpha\sin\gamma & \cos\alpha\sin\beta\sin\gamma + \sin\alpha\cos\gamma & \cos\alpha\cos\beta \end{bmatrix} \tag{2}$$

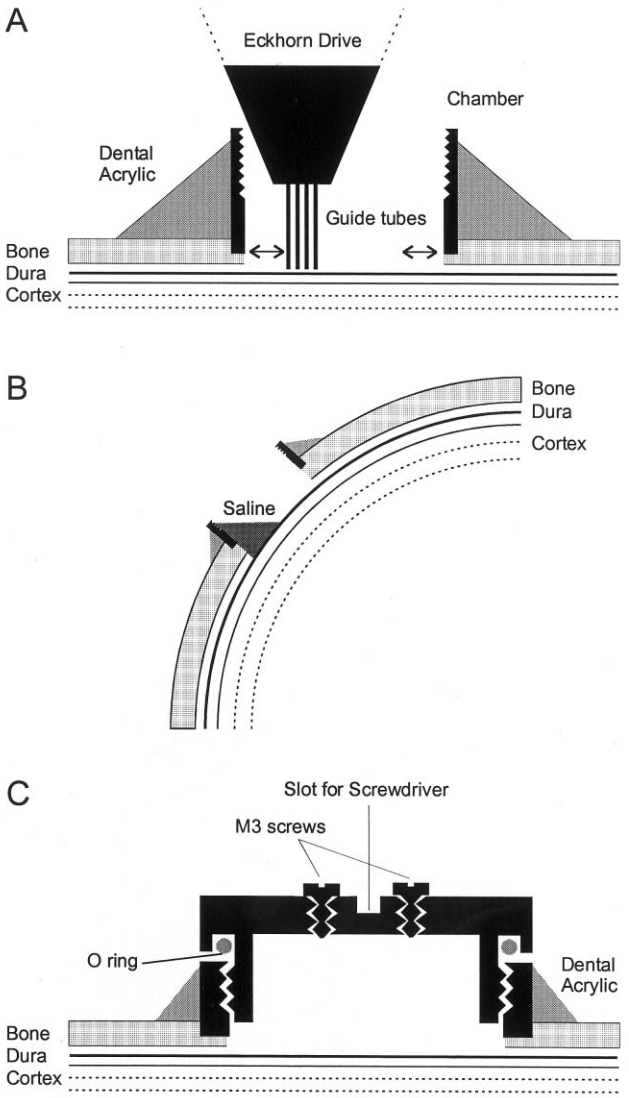

Fig. 2. Problems associated with the conventional design of recording chamber when using the Eckhorn drive. (A) The relatively tall sides of a conventional recording chamber obstruct the head of the Eckhorn recording drive, such that the electrodes cannot penetrate the dura close to the edge of the chamber (area marked with arrows). (B) A smaller recording chamber overcomes this problem, but when placed at an angle on the head (as is necessary to record from primary motor cortex, for example), fluid within the chamber does not cover the dura. This can lead to dural desiccation. (C) A design of recording chamber to overcome these problems. The chamber is in two pieces. A lower, thin ring is attached to the skull with dental acrylic; it is seated down into the bone, preventing obstruction of the Eckhorn microdrive. A cap screws into this ring; a seal is formed with an 'O' ring. The chamber can then be filled with saline through the holes in its top. These are then closed with the M3 screws as shown.

where α, β, and γ are the angles of the co-ordinate axis rotations. Eq. (1) hence has six unknowns: these three angles, and the three components of $\underline{k}$.

The three co-ordinate planes of stereotaxic space are defined from the eye and ear markers in the usual way. The height and anterior-posterior co-ordinates of the ear bars, and the height of the eye markers, are all zero. The midline is determined by careful inspection of structures such as the corpus callosum; a point chosen by eye as lying in the midline has a medio-lateral stereotaxic co-ordinate of zero. Seven of the stereotaxic co-ordinates of these five points are therefore known. Eq. (1) applied to all five points therefore reduces to a set of seven simultaneous equations with six unknowns; a solution must therefore exist.

This solution is easily computed using a spreadsheet in the 'Excel' software package (Microsoft Ltd). The unknowns begin at arbitrary starting values. An error term is defined as the sum of the square of the deviation of each calculated stereotaxic co-ordinate from its known value. This error is minimised by optimising the unknowns. As a check that no mistakes have been made in data entry or in problem definition, the final stereotaxic co-ordinates of the eye and ear bars can be examined. They should be approximately symmetric about the midline, and correspond to reasonable values.

Once the angles and components of $\underline{k}$ have been defined, the transformation of Eq. (1) can be applied to other points measured from the images to determine their location in stereotaxic space. In this way, the location of sulci and other features of interest may be mapped.

A spreadsheet implementing the above optimisation and transformation is available from the authors.

3. Head fixation, drive fixation and recording chamber

In most single-unit recording systems, a lightweight microdrive is directly fixed to an implanted chamber, mounted over the area from which recordings are to be taken. The chamber also serves to protect the area between recording sessions (Lemon, 1984). Such an arrangement has the advantage that if the head moves slightly, the drive will move with it and recording stability will not be compromised. The substantial weight of the Eckhorn drive (approx. 2 kg) means that it cannot be supported by attachment to the chamber. Instead, it is necessary to mount the drive on the primate chair, and to fix the head separately to the same chair. Both of these attachments must be rigid, otherwise relative movement will prevent stable recordings. We have many years of experience using a stainless steel headpiece, custom-made for each monkey and rigidly attached to the skull by a specially designed system of head bolts (see Lemon, 1984 for details). We have integrated this design into the head fixation system by using a circular metal 'halo'. This fits over three threaded 'horns' on the headpiece and is then bolted down to a solid, 50 mm thick steel plate rigidly fixed to the top of the monkey chair. This plate is held in a steel frame, to which the Eckhorn drive can be attached. Using such an arrangement, we have encountered no

problems with recording stability, even when recording from small neurones in superficial cortical layers.

The electrodes in the Eckhorn drive emerge from protective guide tubes; the arrangement of these guide tubes determines the geometry of the relative positions of the 16 electrodes. The length of the guide tubes below the end of the drive is 8 mm. In order to position the tips of the guide tubes just above the exposed dura, to allow electrode penetration, the recording chamber edges must not rise above the dura by more than this amount (see Fig. 2A). However, use of such a shallow chamber poses problems when it is placed at lateral locations on the head, (e.g. for recordings from the hand area of primary motor or lateral premotor cortex). At such locations, the steep angle of the shallow chamber to the horizontal plane will not allow it to contain sufficient fluid to cover the exposed tissue (Fig. 2B), and this will result in desiccation of the dura, and potentially of the cortex below. Accordingly, we have designed a special chamber, illustrated in Fig. 2C, which combines a shallow base, fixed to the skull, and a tall lid, sufficiently large to contain enough fluid to circumvent this problem.

The chamber is constructed of implantable grade stainless steel, and is in two parts. The lower part consists of a ring, 1.5 mm thick and 4 mm high, having 12 mm internal diameter. The inside of this ring is threaded. The ring is implanted onto the skull over the craniotomy. The bone underneath the ring is thinned using a dental drill to permit the top of the ring to be closer to the dura. The ring is attached to the skull using dental acrylic; the outside of the ring has vertical indentations cut into it every 45° to provide better attachment of the acrylic, and to prevent the ring from turning. The acrylic is anchored to the bone using miniature skull screws (4.7 mm long, shaft diameter 1.17 mm; Fine Science Tools). On the upper surface of the ring are three round indentations, made with a 1 mm drill; these are used as triangulation points to provide reproducible location of the drive relative to the chamber in each session.

The upper half of the chamber (the lid) can be screwed down into the ring using a screwdriver inserted into the slot on its top. An 'O' ring, held within a groove in the cap, provides a seal. In the top of this cap are two M3 threaded holes. Once the cap is tightened onto the ring, the chamber can be filled with saline through these using a hypodermic syringe fitted with a blunt needle. The holes are then sealed with two short M3 screws.

Using this arrangement, the tissue within the chamber is kept moist and sterile in between recording sessions, whilst permitting good access to the craniotomy during recordings. An advantage of such a low profile chamber is that it is possible to view the penetration of the electrodes through the dura using a binocular microscope; this provides valuable information on the current thickness of the dura.

4. Care of the dura mater

After a craniotomy is made in the skull, scar tissue begins to accumulate over the exposed dura mater. At first this is a filamentous growth; it rapidly toughens, and vascularises. Conventional tungsten or platinum-iridium microelectrodes which are used in single electrode recording studies in conscious animals (Lemon, 1984) have a typical shaft diameter of 150 μm. In spite of the tissue growth over the dura, these electrodes remain capable of penetrating into the cortex for 1–2 months following the implant surgery. However, although penetration is possible, it causes increasing dimpling of the dura before the electrodes will enter. Such dimpling can produce transient spreading depression in the cortex, and impair subsequent recordings.

The Eckhorn system uses 80 μm diameter electrodes, and penetration with such thin electrodes is impossible if there is significant scar tissue growth. If the dura is untreated, our experience is that successful penetrations can be made for at most a week after the implant. Regular surgeries are then required to strip the accumulated tissue; these can be very time consuming because the highly vascular nature of the growth requires careful haemostasis. These surgeries interrupt the routine of chronic recordings, and adversely effect the performance of the animal on the behavioural task.

In order to overcome these problems, we have developed a protocol to prevent the build up of tissue on the dura without the need for regular surgeries under general anaesthesia. Each day, at the end of the recording session, the experimenter removes accumulated tissue whilst working under a binocular microscope, using fine watchmakers' forceps, a corneal hook, and miniature surgical scissors. If this is performed daily, it is our experience that the animal usually shows no signs of discomfort as the fine growth is removed, presumably because it is not yet innervated. However, should dura 'picking' or 'scraping' distress the animal, the dura should first be covered with a layer of local anaesthetic cream (EMLA, Astra Pharmaceuticals Ltd); after a few minutes to allow it to infiltrate the tissue, the cream should be aspirated. The tissue growth can then be removed without pain. The use of local anaesthetic is most often necessary when working close to a large dural blood vessel (e.g. middle meningeal artery). Dural nociceptive fibres are known to be positioned predominantly close to such vessels (Wolff, 1963).

Tissue re-growth can be reduced using the antimitotic agent, 5-flurouracil (5-FU), which acts by retarding mitosis of fibroblasts (Cordeiro et al., 1997). A saturated solution is made up using a 250 mg aliquot of 5-FU powder (Sigma Chemicals Ltd) and 10 ml of sterile saline, mixed using a magnetic stirrer at room temperature. It is important to note that 5-FU is a highly carcinogenic compound. It is particularly dan-

gerous in the powdered form, and the mixing of the solution should be performed in a fume cupboard. At all times when working with either the powder or the solution, gloves, eye protection, a mask, and a lab coat should be worn. The solution appears to retain its effectiveness for several weeks.

After the tissue overlying the dura has been removed, the anti-mitotic solution should be applied. Later (5 min), the solution should be removed, and the dura thoroughly rinsed with sterile saline. Care must be taken not to allow any anti-mitotic to spill onto the skin of the animal. The most effective method of achieving this is using an aspirator connected to a suction pump; this also ensures that all traces of the anti-mitotic are washed away. Anti-mitotic treatment is best carried out daily, although it is useful even at less frequent intervals. It should first be applied during the implant surgery when the craniotomy is made, as this is likely to be the time of maximum scar tissue formation.

Two drops of antibiotic (an ophthalmic eye drop preparation is convenient, e.g. Genticin, Roche; Ciloxan, Alcon-Couvreur) should then be placed on the dura, and the chamber sealed as described above.

Using the above procedure, the dura can be maintained in a soft condition, suitable for penetration by the fine electrodes of the Eckhorn system, for many weeks without the need for a surgery under general anaesthesia. An additional advantage is that even if some growth does occur, this is considerably less vascular than if there is no anti-mitotic treatment. Dura strip surgeries, when necessary, are therefore much more straightforward.

We have used 5-FU in the manner described above continuously for periods of months in a single chamber. We have seen no ill effects on the animal's health; it seems highly unlikely that appreciable quantities of the compound enter the systemic circulation given the short duration of exposure each day. Single unit recordings from the cortex underlying dura so treated have shown normal patterns of task dependence, and in all ways appeared normal.

5. Multiple electrode recording system

Two principle methods exist for making multiple simultaneous recordings in the brain. The first uses chronically implanted electrodes, such as fine microwires (e.g. Nicolelis et al., 1997), which cannot be moved once implanted. The second uses electrodes which are inserted transdurally afresh each day, and moved to locate the desired cellular activity. The former method has the advantage that no time must be spent at the start of a recording session in tracking to find suitable recordings. By contrast, the ability to move the electrodes makes it possible to search for particular types of neurone. Since in our experiments we wished to record antidromically identified single units, we chose to use the Eckhorn microdrive which has 16 independently moveable electrodes. We have found that a tip impedance of 1.5–4 MΩ yields clean single unit recordings in the primary motor cortex and other frontal motor areas.

A considerable problem encountered in using the Eckhorn drive (or others like it) is how to achieve simultaneous control of so many different electrodes. A single experimenter is not capable of performing the information processing required. In order to overcome this, we have computerised much of the control of the experimental system as shown in Fig. 3. A 'Master' personal computer controls the electrode movement and the stimulator, and displays spike activity from all electrodes, using software operated through a graphical user interface (GUI). Digitisation of spike activity is achieved using a CED 1401+ interface. In addition, two of the channels can be selected for display on a dual beam oscilloscope, and to stereo headphones, for audio monitoring. The software is designed to place all GUI controls for one electrode close together on the screen, next to the display of the signal from that electrode. Mistakes involving the user confusing channels are thus avoided. This computer is fitted with a touch screen interface for rapid operation of the program.

Even with such a system, it is still our experience that a single experimenter can monitor activity successfully on only around three electrodes at once. The solution to this is straightforward but costly: more experimenters must be involved in the recordings. Each additional experimenter uses a 'Slave' computer. These communicate with the 'Master' via a fast (100 Mb/s) switched Ethernet link. They receive sampled waveforms from the electrodes for display, and can control the movement of any electrode, using software similar to that running on the 'Master'. The 'Slave' workstations can also control monitoring of two selected spike waveform channels via an oscilloscope and headphones.

Use of a 'Master-Slave' configuration permits 'Slaves' to be configured differently to perform different roles, so long as all adhere to the same standards in communicating with the 'Master'. We have made use of this flexibility in our recordings to program one of the Slave PCs to advance multiple electrodes automatically, whilst scanning the responses following pyramidal tract stimulation for the presence of antidromically activated cells. The electrodes are advanced in small steps sequentially to avoid the tissue drag which could be caused by moving many electrodes together. The detection algorithm running on this 'Slave' computer calculates the mean and standard error of the response waveform recorded on each electrode following pyramidal tract stimulation. A colour display shows if any points have

a mean deflection significantly different from zero. An antidromic response is assumed to be present if more than a threshold number of contiguous bins show a significant deviation. Once a pyramidal tract neurone (PTN) is so detected, the automated 'Slave' stops moving that electrode, and its control is taken over by an experimenter who fine tunes the electrode position to obtain the optimal recording. This technique permits a shortening of the time taken to find cells on all electrodes before recordings can begin.

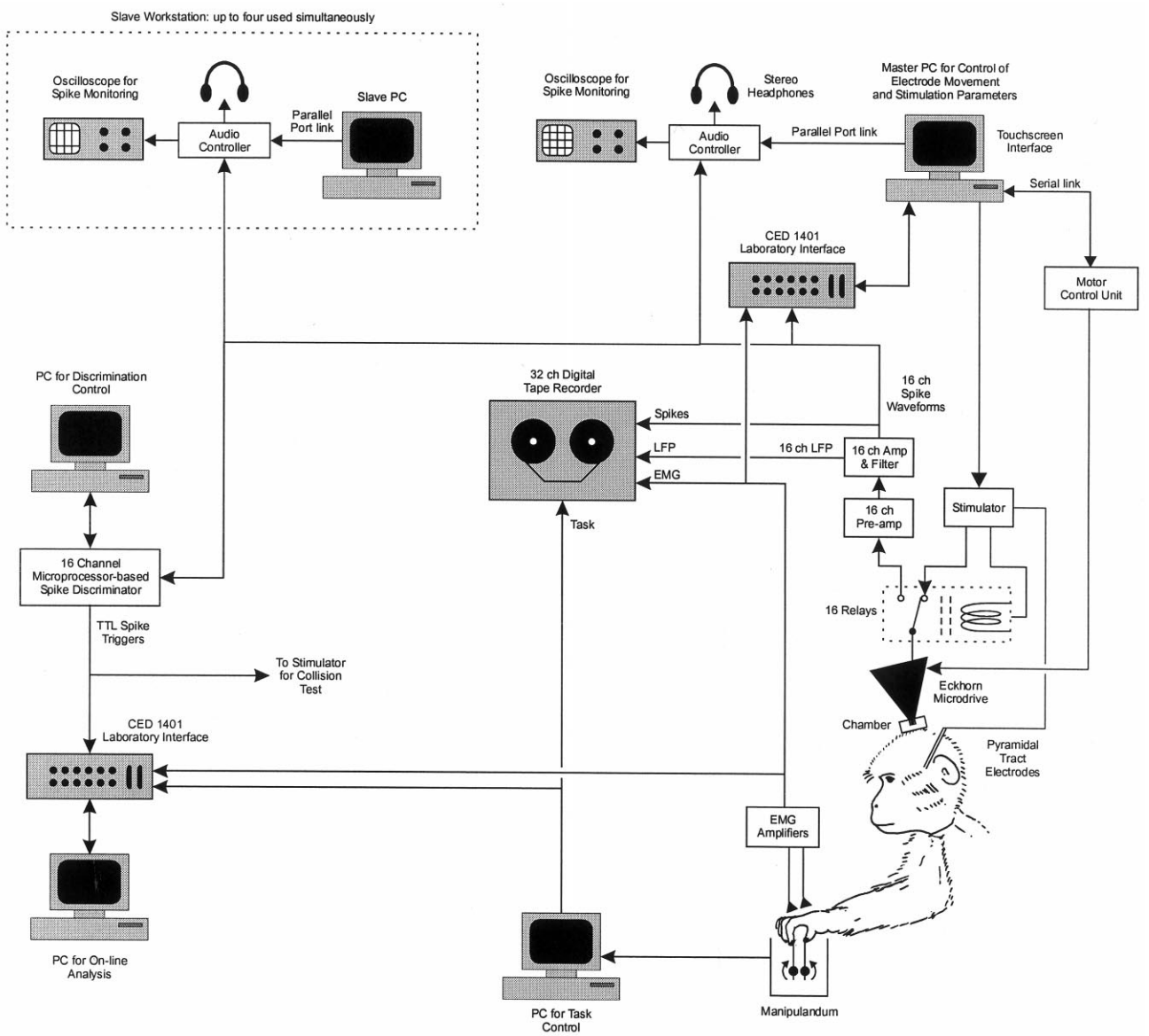

Fig. 3. Schematic of the system, based on the Eckhorn 16 electrode drive, used to make multiple simultaneous single unit recordings from awake behaving monkeys. At the heart of the system is the 'Master' PC (top right). This controls stimulation parameters using the custom built stimulator. The stimulator switches the electrodes between record and stimulate mode using relays built into the pre-amplifiers. The 'Master' PC also controls electrode movement. Waveforms from the recordings are sampled by the CED 1401 A/D interface, and displayed. Finally, this PC controls which of the 16 signals are routed to stereo headphones for audio monitoring, and to a dual beam oscilloscope. The 'Slave' PCs (top left) communicate with the 'Master' via a fast Ethernet link. Operators of these computers can move electrodes, view waveforms recorded from electrodes, and monitor two of the spike channels using their own headphones and oscilloscope. On-line spike discrimination is handled by a dedicated PC (middle left) and micro-processor based system. Discrimination parameters are set from either the spike discrimination PC, or from the 'Slave' PCs which communicate with the discriminator PC over the Ethernet link. This permits multiple users to control discrimination parameters. However, on-line discrimination is still considered unreliable, and the trigger pulses which it produces are not saved for later analysis. On-line discrimination *is* used for on-line spike triggered averaging and task response averaging, which is performed by a dedicated PC and 1401 laboratory interface (bottom left). On-line discrimination pulses are also needed for the collision test, which permits antidromic identification. One PC (middle bottom) controls the behavioural task, which in our experiments requires production of a precision grip. All signals, including spike waveforms, local field potential (LFP), EMG, and task markers, are recorded on a 32 channel tape recorder (centre of figure) for off-line analysis.

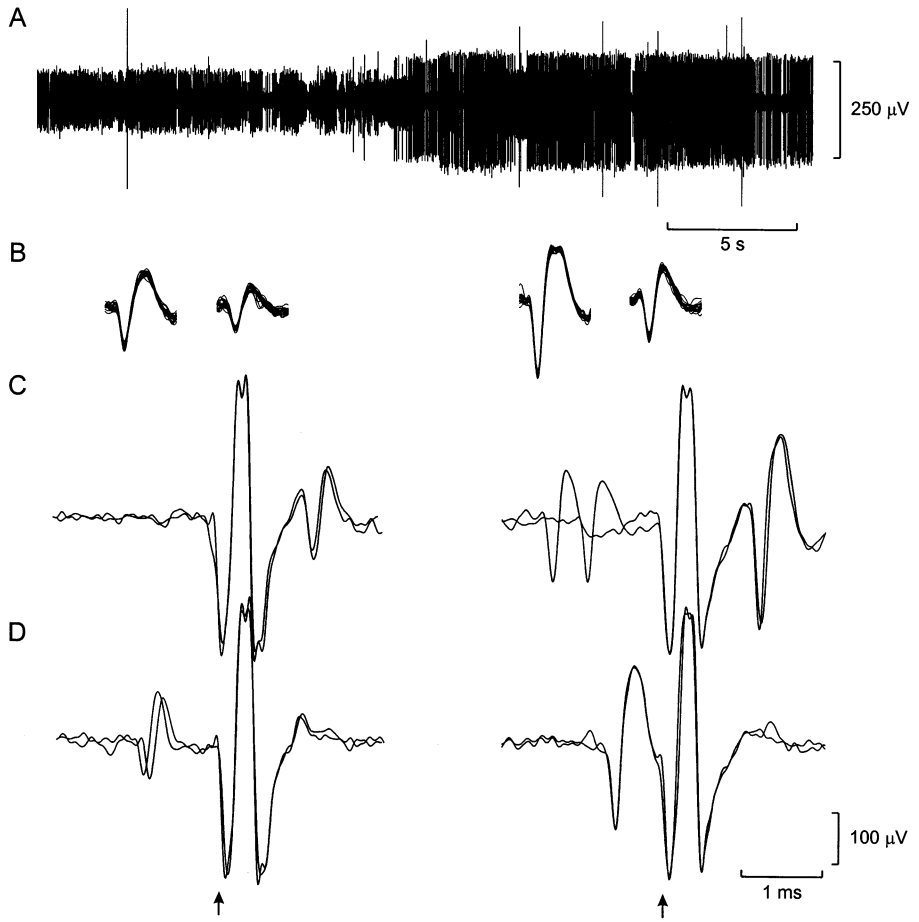

Fig. 4. Benefits of antidromic identification. (A) Recording from a single electrode using the Eckhorn system in the motor cortex of an awake behaving monkey. Around halfway through the period illustrated, slippage of the electrode relative to the tissue occurred, leading to an abrupt shift in the form of the recorded activity. (B) Twenty overlain spikes from two neurones, discriminated from this electrode's recording on the basis of differences in the size and shape of their action potentials. (C) Two overlain traces of the response in this recording to stimulation through the pyramidal tract electrodes at 250 μA. An antidromic response can be clearly seen following the stimulus artefact. The threshold for this antidromic response was 110 μA in both cases. (D) Collision of the antidromic response by triggering the stimulus by a spontaneous spike. Collision occurred at spike-to-stimulus intervals up to 0.9 ms in both cases. In (B–D), traces on the left were derived from the recording before the abrupt change; those on the right after it. Scale bars for (B–D) are the same. Arrows mark the onset of the pyramidal tract stimulus. Comparison of the spontaneous trigger spikes of (D) with those in (B) shows that the largest cell in the record in each case was the same antidromically identified PTN.

After clear single unit activity has been located on as many channels as possible, single unit spike trains are discriminated into TTL trigger pulses using a microprocessor-based unit. The microprocessors implement a double amplitude-time window algorithm in real time. The window locations and sizes are transmitted to the discriminator from a dedicated computer, which runs custom software allowing these parameters to be set interactively by the user. This computer communicates with the 'Slave' workstations via fast Ethernet, so that spike discrimination parameters for a given channel can also be set from any of the 'Slaves'.

The aim of such discrimination is to permit on-line characterisation of the units, and particularly to provide triggers for the collision tests which are needed to identify PTNs (Lemon, 1984; see Fig. 4). A further dedicated PC samples discriminated spike times, the times of task events, and EMG, using a CED 1401 + interface. Software on this computer displays spike-triggered averages of rectified EMG (Fetz and Cheney, 1980; Lemon et al., 1986), permitting on-line identification of cortico-motoneuronal cells, important for our experimental aims. Inter-spike interval histograms are also displayed; the absence of any discharges falling within the first millisecond of these histograms is taken as evidence of clean single unit discrimination. Finally, the relationship of the unit firing to the task is displayed.

Whilst on-line discrimination is useful, it can never be entirely reliable, as a result of the many demands on the experimenters during the recording which prevent them from paying full attention to optimal adjustment

of the discrimination parameters. Therefore we do not record the on-line discriminated pulses, but instead save the entire spike waveform from all recorded channels to a 32 channel digital tape recorder (TEAC RX-832) sampling at 24 kHz per unit channel. EMG activity and signals related to task performance are also recorded, as are local field potentials (LFP) from all channels.

Following a recording session, the digitised data is transferred from the tape recorder directly to the hard disc of a PC using a SCSI interface. Spike waveform files are separated into the times of single unit firings using custom-written software which uses a waveform clustering approach (Eggermont, 1990). If the discriminated waveforms appear consistent in size and shape, and there are no spikes in the first millisecond of the inter-spike interval histogram, the spikes are assumed to come from an uncontaminated single unit and the times of occurrence are written to files for later analysis.

Using such 'cluster cutting' techniques, it is often possible to separate several cells whose discharges have been recorded on the same electrode (see Lewicki, 1998 for a review). However, it must be emphasised that however sophisticated the discrimination software, single units cannot be isolated from noisy recordings in which many similarly sized cells are present. It is much more efficient in terms of experimenter time, and ultimately yields better quality data, if recordings are not commenced until all operators are certain of the discriminability of units on their channels. This can be greatly aided by viewing spikes on a fast oscilloscope, by audio monitoring, and by using the on-line spike discriminators. Once recordings are begun, it is likewise important that all channels continued to be monitored. Should the quality of a given recording begin to deteriorate, it can often be improved by small (c. 10 μm) movements of the electrodes. Such movements probably help to compensate for tissue slippage relative to the electrode. Careful attention to such monitoring during the experiment renders the off-line spike discrimination straightforward and rapid.

6. Antidromic identification in multiple electrode recording

In many single unit studies, the cells recorded are essentially randomly selected, with a bias towards recording larger neurones (Towe and Harding, 1970; Humphrey and Corrie, 1978). Although of use in characterising area population responses (e.g. Mushiake et al., 1991), this approach suffers from a lack of information on the functional role of each neurone within the cortical network. The method of antidromic activation permits the identification of neurones which project axons along a given fibre tract (Lemon, 1984). The activity of the cells during behavioural tasks may then be interpreted in the light of their known projections. In our recordings, we have placed electrodes in the pyramidal tract at the level of the medulla (see Lemon, 1984), and used antidromic following to stimulation through these electrodes to identify PTNs.

Searching for identified neurones might appear to be much more difficult than working with unidentified cells. Many times a cleanly discriminable unit is rejected because it is not a PTN, and this could decrease the recording yield. However, in the frontal motor areas (Dum and Strick, 1991) PTNs are sufficiently frequently encountered that this is not a serious disadvantage.

In fact, we have found working with identified cells to have distinct advantages in *improving* recording yield. If the animal makes a sudden or unusually large movement, recordings will often show abrupt changes in the size and form of action potentials. If the cells are unidentified, it is not possible to have confidence following such an occurrence that the same cells are present in the record as were seen previously. This results in the abandonment of a recording session halfway through collection of a full set of data. By contrast, if the cells were antidromically identified prior to the sudden change, all that is necessary is briefly to switch on the pyramidal tract stimulus and re-confirm the antidromic responses. If the neurones' 'signature' of threshold, antidromic latency and collision interval (see Lemon, 1984, for full details) corresponds to the values measured earlier, the recording session can proceed with high confidence that, whatever has happened to the size or shape of the action potentials, the same cells are present.

An example of such a situation is provided by Fig. 4. During the period of recording shown by Fig. 4A, a sudden slippage of the electrode relative to the tissue occurred, possibly because of a large movement by the animal. This caused an increase in the size of the recorded spike activity. Fig. 4B shows that both before, and after, this event, two clean single units could be discriminated from the electrode on the basis of the size and shape of their action potentials. It was, however, not clear which cell was which following the abrupt change. Fig. 4C shows that one of the cells responded antidromically to stimulation of the pyramidal tract electrodes before and after the slippage. Fig. 4D shows the effect of triggering the stimulus by a spontaneous spike, discriminated to come from the largest action potential in the record. The spontaneous orthodromic spike collided with the stimulus-evoked antidromic spike in the axon between the cortex and the pyramids, so that no antidromic response was seen. This collision test proves that the triggering spike in the record in each case was a PTN. The latency, threshold and collision interval for the antidromic identification were identical before and after the amplitude change. The

largest spike in the recording before and after the tissue slip must therefore have come from the same cell.

This test can be used rapidly across many simultaneously recorded channels, making it invaluable in multiple single unit recording. Events as illustrated in Fig. 4A are generally unavoidable in work on awake behaving animals. In addition, the collision test is a completely unambiguous means of confirming that the discriminated spikes do originate from the antidromically identified neurone, and are not contaminated by activity from other cells.

7. Correction for non-stationarities in correlation measures

One of the principle reasons for recording multiple single neurones simultaneously is to permit cross-correlation of their discharge, thereby permitting the detection of short-term synchrony (Perkel et al., 1967; Sears and Stagg, 1976). However, this is made more complex by the fact that the firing rates of the neurones concerned are often non-stationary. In awake behaving animals performing behavioural tasks, neural firing rates can modulate by more than 100 Hz. The usual approach to correcting for this is to compute a shift predictor by comparing spike trains across trials (Perkel et al., 1967); this assumes that the modulation in firing rate has a constant profile from one trial to the next. However, there are often large trial-by-trial variations in firing rate. If the variations in firing rate covary between two neurones from trial to trial, this will lead to a peak in their cross-correlation histogram which will not be present in the shuffle predictor, even if they exhibit no short-term synchronisation (Pauluis and Baker, 1999; Brody, 1999a,b).

In order to correct for such effects, we have developed a novel means of determining the instantaneous discharge rate of a neurone (Pauluis and Baker, 1999). The technique is summarised in Fig. 5. From the discharge of the neurone (Fig. 5A), the raw firing rate is computed as the reciprocal of the inter-spike intervals (ISIs, Fig. 5B). This measure is highly variable, reflecting the variability in ISIs, and clearly needs to be smoothed to produce a useful measure.

Such smoothing usually requires a trade-off between under-smoothing, producing a variable measure, and over-smoothing, which will blur details of the rate modulation. To avoid this, we firstly explicitly detect points of rapid firing rate change (arrows, Fig. 5B). The ISIs are assumed to follow a gamma distribution, which provides for a relative refractory period, and is thus a better representation of the interval statistics of a neurone than the more commonly used Poisson process. Using the gamma distribution, if the probability of two successive ISIs being smaller than the observed values is calculated to be less than 0.05, a rate change point is marked. The firing rate estimate is then smoothed by convolution with a Gaussian kernel (standard deviation 20 ms), but the smoothing is not carried out across the points of explicitly detected rate change. This provides an estimate of the instantaneous firing rate of the neurone which varies smoothly between rate change points, but abruptly at them (Fig. 5C). Although it closely follows the firing rate modulation, this measure contains no temporal information about the precise timing of individual spikes. For more details of the implementation of this procedure, including corrections for the effect of binning and for the intrinsically delayed response which an integrate and fire neurone gives to a change in its inputs, see Pauluis and Baker (1999).

Such an instantaneous firing rate measure can be of great use in producing a prediction of the cross-correlation between two neurones on the null hypothesis that they exhibit no short-term synchronisation. This is achieved simply by computing the analogue cross-correlation of the two cells' instantaneous discharge probability. Fig. 5D shows an example of cross-correlation histograms for two pairs of neurones, with the overlaid predictor computed in this way. These cells were recorded from monkey primary motor cortex using the Eckhorn system whilst the animal performed a precision grip task. It can be seen that the predictor follows the broad modulation of the cross-correlation histogram closely; however, the central, sharp peak in each case is not reproduced. The dotted lines mark 95% confidence limits. These are calculated as:

$$P(t) \pm 2\sqrt{P(t)} \tag{3}$$

where P represents the cross-correlation predictor; this assumes that the expected number of counts per bin is sufficiently large that the normal approximation to the Poisson distribution is valid. For both cells, the central peak exceeds these limits, indicating the presence of short-term synchronisation superimposed on the co-modulation of firing rate which has a broader time course.

The instantaneous firing rate technique can also be applied to the removal of non-stationarities from spike triggered averages (STA) of rectified EMG (Fetz and Cheney, 1980; Lemon et al., 1986). The STA technique is useful for the identification of cells which project monosynaptically to the motoneurones innervating the muscle whose EMG is averaged. Such monosynaptic connections lead to a post-spike facilitation (PSF) with peak width at half maximum height smaller than 7 ms (Baker and Lemon, 1998). Experimentally, STAs can often be difficult to interpret because of a non-stationary baseline. Previous work has fitted a regression line to this and subtracted it (Bennett and Lemon, 1994);

this however requires a subjective decision on the baseline region to be used for the fitting, and cannot compensate for non-linear baseline variations. Use of shuffle predictors produces highly inaccurate predictors as a result of the variability of EMG from trial to trial (Baker, unpublished observations).

The instantaneous discharge probability method conveniently solves these problems. The analogue cross-correlation computed between the instantaneous firing rate and the rectified EMG provides an accurate predictor of the STA on the null hypothesis of no short-term synchronisation between triggering cell and the EMG. Fig. 5E shows an example of two STAs overlain with such a predictor. The dotted lines represent approximate 95% confidence limits, calculated as twice the standard error assessed from the STA. In each case, the non-stationarity of the baseline is mimicked by the predictor, but the brief PSF at a latency of around 10 ms is not. Both PSFs are statistically significant. These two peaks have a peak width at half maximum of 3.6 and 3.2 ms respectively, indicating that the triggering cells are likely to make monosynaptic connections to the motoneurones innervating the muscles whose EMG is averaged (Baker and Lemon, 1998). In the example

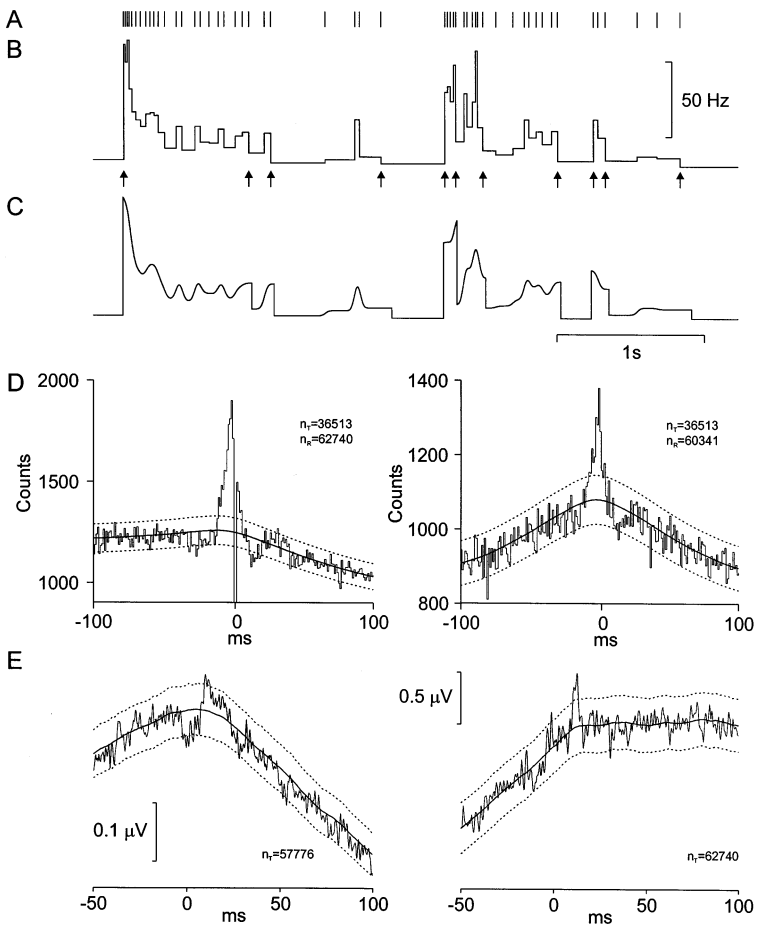

Fig. 5. Prediction of correlation measures using instantaneous discharge probability estimates. (A) Example of a spike train, from an identified pyramidal tract neurone (PTN) recorded in an awake behaving monkey. (B) Raw estimate of instantaneous firing rate, produced as the reciprocal of the inter-spike intervals (ISIs). Points of rapid change in firing rate are detected by a probabilistic algorithm, and are marked by the arrows. (C) The firing rate estimate is smoothed by convolution with a Gaussian kernel (standard deviation 20 ms). Smoothing is not carried out across the detected points of rapid rate change, producing a measure which varies smoothly between change points and abruptly at them. (D) Examples of cross-correlation histograms between pairs of motor cortical PTNs. Overlain on the histograms are the cross-correlations of the instantaneous discharge probability estimates for the cells pairs. The latter serve as predictors for the shape of the histograms, on the null-hypothesis of no short-term synchronisation between the cells. Dotted lines indicate 95% confidence limits around the predictors. The left histogram was compiled from two cells whose discharge was recorded on the same electrode and separated according to differences in the size and shape of action potentials. Overlapping spikes could not be detected; accordingly, the central bin artefactually has zero counts. Central peaks, indicative of common synaptic input to the two neurones, clearly rise above the confidence limits. Bin width 1 ms. (E) Spike triggered averages of rectified EMG from the adductor pollicis (left) and extensor carpi radialis muscle (right) compiled using two different PTNs in the motor cortex as triggers. Overlain is a predictor formed by cross-correlating the cells' instantaneous discharge probability estimate with the rectified EMG. Dotted lines mark approximate 95% confidence limits, derived as described in the text. Post-spike facilitations rise above significance in each case: n_T, number of trigger spikes; n_R, number of response spikes.

on the left of Fig. 5E, the narrow PSF is superimposed on a broader peak which probably reflects pre-synaptic synchronisation amongst CM cells in the cortex (Baker and Lemon, 1998). Interpretation of these traces is made considerably more straightforward by the availability of an accurate corrector for the non-stationarity of the STA baseline.

Acknowledgements

The authors wish to thank Dr Chris Seers for technical support, and Mr Uwe Thomas and Mr Dirk Hoehl of Thomas Recording Ltd for help and advice on the Eckhorn system. Dr Jeff Keating provided critical comments on an earlier version of this manuscript. Funded by the Medical Research Council, the Wellcome Trust and the Brain Research Trust.

Appendix A. Contact information for suppliers

EMLA local anaesthetic cream
Astra Pharmaceuticals Ltd,
Kings Langley,
Hertfordshire WD4 8DH,
UK.

5-fluorouracil (Antimitotic Agent)
Catalogue number F-6627,
Sigma Chemicals Ltd,
Fancy Road,
Poole,
Dorset BH17 7NH,
UK.
Tel.: +44-800-373731

Corneal sharp angled hook (Product no. 10063-15)
Miniature self-tapping bone screws (Product no. 19010-00)
0.9 mm dental burr, used to drill pilot holes for the above screws (Product no. 19007-09)
Fine Science Tools,
Interfocus Ltd,
14–15 Spring Rise,
Falconer Road,
Haverhill,
Suffolk CB9 7XU,
UK.
Tel.: +44-440-703460

1401+ Interface
Cambridge Electronic Design,
Science Park,
Milton Road,
Cambridge,
UK.
Tel.: +44-1223-420186
http://www.ced.co.uk

Eckhorn System and Electrodes
Thomas Recording,
Marburger Strasse 30/50,
35043 Marburg,
Germany.
Tel.: +49-6421-46442
http://home.t-online.de/home/ThomasRecording

References

Baker SN, Lemon RN. A computer simulation study of the production of post-spike facilitation in spike triggered averages of rectified EMG. J Neurophysiol 1998;80:1391–406.

Bennett KMB, Lemon RN. The influence of single monkey corticomotoneuronal cells at different levels of activity in target muscles. J Physiol 1994;477:291–307.

Brody CD. Correlations without synchrony. Neural Comp 1999a;11(15):1537–51.

Brody CD. Disambiguating different covariation types. Neural Comp 1999b;11:1527–35.

Cordeiro MF, Occlestone NL, Khaw PT. New concepts: manipulation of the wound-healing response. Dev Opthalm 1997;28:242–60.

Dum RP, Strick PL. The origin of corticospinal projections from the premotor areas in the frontal lobe. J Neurosci 1991;11:667–89.

Eckhorn R. Oscillatory and nonoscillatory synchronizations in the visual-cortex and their possible roles in associations of visual features. Prog Brain Res 1994;102:405–26.

Eckhorn R, Thomas U. A new method for the insertion of multiple microprobes into neural and muscular tissue, including fiber electrodes, fine wires, needles and microsensors. J Neurosci Methods 1993;49:175–9.

Eggermont JJ. The Correlative Brain. Theory and Experiment in Neural Interaction. Berlin: Springer-Verlag, 1990.

Eggermont JJ, Epping WJM, Aertsen AMHJ. Stimulus dependent neural correlations in the auditory midbrain of the grassfrog (*Rana temporaria* L.). Biol Cybern 1983;47:103–17.

Fetz EE, Cheney PD. Postspike facilitation of forelimb muscle activity by primate corticomotoneuronal cells. J Neurophysiol 1980;44:751–72.

Flecknell P. Laboratory Animal Anaesthesia. London: Academic Press, 1996:27–49.

Humphrey DR, Corrie WS. Properties of pyramidal tract neuron system within a functionally defined subregion of primate motor cortex. J Neurophysiol 1978;41:216–43.

Jasper H, Ricci GF, Doane B. Patterns of cortical neurone discharge during conditioned motor responses in monkeys. In: Wolstenholme G, O'Connor C, editors. Neurological Basis of Behaviour. Boston: Little Brown, 1958.

Kilner JM, Baker SN, Salenius S, Jousmäki V, Hari R, Lemon RN. Task-dependent modulation of 20–30 Hz coherence between rectified EMGs from human hand and forearm muscles. J Physiol 1999;5-6:559–70.

Lee D, Port NL, Kruse W, Georgopoulos AP. Variability and correlated noise in the discharge of neurons in motor and parietal areas of the primate cortex. J Neurosci 1998;18:1161–70.

Lemon RN. Methods for neuronal recording in conscious animals. In: Smith AD, editor. IBRO Handbook Series: Methods in Neurosciences, vol. 4. London: Wiley, 1984:1–162.

Lemon RN, Mantel GWH, Muir RB. Corticospinal facilitation of hand muscles during voluntary movement in the conscious monkey. J Physiol 1986;381:497–527.

Lewicki MS. A review of methods for spike sorting: the detection and classification of neural action potentials. Network: Comput Neural Syst 1998;9:R53–78.

Lindsey BG, Hernandez YM, Morris KF, Shannon R, Gerstein GL. Dynamic reconfiguration of brain stem neural assemblies: respiratory phase-dependent synchrony versus modulation of firing rates. J Neurophysiol 1992;67:923–30.

Mushiake H, Inase M, Tanji J. Neuronal activity in the primate premotor, supplementary, and precentral motor cortex during visually guided and internally determined sequential movements. J Neurophysiol 1991;66:705–18.

Nicolelis MA, Ghazanfar AA, Faggin BM, Votaw S, Oliveira LM. Reconstructing the engram: simultaneous, multisite, many single neuron recordings. Neuron 1997;18:529–37.

Pauluis Q, Baker SN. An accurate measure of the instantaneous discharge probability, with application to unitary joint-event analysis, Neural Comput 1999;in press.

Perkel DH, Gerstein GL, Moore GP. Neuronal spike trains and stochastic point processes. II. Simultaneous spike trains. Biophys J 1967;7:419–40.

Riehle A, Grün S, Diesmann M, Aertsen A. Spike synchronization and rate modulation differentially involved in motor cortical function. Science 1997;278:1950–3.

Sears TA, Stagg D. Short-term synchronization of intercostal motoneurone activity. J Physiol 1976;263:357–81.

Singer W, Gray CM. Visual feature integration and the temporal correlation hypothesis. Annu Rev Neurosci 1995;18:555–86.

Stopfer M, Bhagavan S, Smith BH, Laurent G. Impaired odour discrimination on desynchronization of odour-encoding neural assemblies. Nature 1997;390:70–4.

Towe AL, Harding GW. Extracellular microelectrode sampling bias. Exp Neurol 1970;29:366–81.

Vaadia E, Haalman I, Abeles M, Bergman H, Prut Y, Slovin H, Aertsen A. Dynamics of neuronal interactions in monkey motor cortex in relation to behavioural events. Nature 1995;373:515–8.

Wolff HG. Headache and Other Head Pain. New York: Oxford University Press, 1963.